Heliyon 8 (2022) e12366

Contents lists available at ScienceDirect

Heliyon

journal homepage: www.cell.com/heliyon

Research article

Effects of multi-mode physical stimulation on APP/PS1 Alzheimer's disease model mice

Shupeng Liu [a,*], Shuyang Li [a], Yudan Xia [a], Heng Zhang [a], Jing Tian [b,**], Chunlei Shan [c], Fufei Pang [a], Ying Wang [d], Yana Shang [a], Na Chen [a,***]

[a] Key Laboratory of Specialty Fiber Optics and Optical Access Networks, Shanghai Institute for Advanced Communication and Data Science, Shanghai University, Shanghai, 200444, China
[b] School of Electron and Computer, Southeast University Chengxian College, Nanjing, 210088, China
[c] School of Rehabilitation Science, Shanghai University of Traditional Chinese Medicine, Shanghai, 201203, China
[d] School of Public Health, Fudan University, Shanghai, 200032, China

ARTICLE INFO

Keywords:
Alzheimer's disease
Amyloid
γ rhythm
APP/PS1
Multimodal physical stimulation

ABSTRACT

Some researchers and clinics have reported that non-drug treatments for Alzheimer disease (AD) such as electrical stimulation, light stimulation, music stimulation, laser stimulation, and transcranial magnetic stimulation may have beneficial treatment effects. Following these findings, in this study, we performed multimodel physical stimulation on APP/PS1 mice using visible light, music with a γ rhythm, and an infrared laser. And the effects of physical stimulation on APP/PS1 mice were evaluated by behavioral analysis, the content of amyloid ($A\beta_{40}$ and $A\beta_{42}$), and NISSL staining of hippocampal tissue slices. The results of subsequent behavioral and tissue analyses showed that the multi-model physical stimulations could relieve APP/PS1 mice's dementia symptoms, such as the behavior ability, the content of Aβ40 and Aβ42 in the hippocampal tissue suspension, and Nissl staining for hippocampal tissue analyses.

1. Introduction

First presented at a meeting in 1906 by Dr. Alois Alzheimer in Tübingen, Germany, Alzheimer's disease (AD) was originally described as "a special and serious disease process in the cerebral cortex." Now, AD is described as a progressive degenerative disease accompanied by cognitive dysfunction, memory loss, and mood disorders. As the international population continues to age, people are paying more and more attention to AD (Jack et al., 2018; Lane et al., 2018; Li et al., 2020). At present, more than 50 million people in the world are affected by dementia, and AD is the most common form of dementia, accounting for about 70% of dementia cases. According to the World Health Organization (WHO) forecast, the world's elderly population will reach 2.02 billion by 2050 (Fulop et al., 2022; Holtzman et al., 2011).

While the pathogenesis of AD is not fully understood, its pathological features are usually senile plaques (SP) formed by β-amyloid (Aβ) and neurofibrillary tangles (NFT) formed by hyperphosphorylated tau protein (Chan et al., 2013; Cheignon et al., 2018; Fonseca et al., 2019; Guo et al., 2020; Haass and Selkoe, 2007). Both features were found more frequently in the cortex and hippocampus of AD individuals than in other elderly individuals. At present, the main neuropathological criteria for diagnosing AD are the presence of senile plaques outside the cells and neurofibrillary tangles in the cells (Lamb et al., 2018; Tyan et al., 2012; Wegmann et al., 2021). In 1991, the pathogenesis of AD was first proposed to be Aβ accumulation (Beyreuther and Masters, 1991), and this amyloid hypothesis has since become the mainstream explanation. Aβ protein was once considered to be the culprit leading to neuronal cell death, and it can indeed cause clinical symptoms such as cognitive dysfunction and abnormal mental behavior in patients (Long and Holtzman, 2019). In addition, Alzheimer's disease can also cause the degeneration of neurons in the temporal lobe and hippocampus (Chiavellini et al., 2022) and glial hyperplasia (Guo et al., 2020), cerebrovascular amyloidosis (Hampel et al., 2020), neuroinflammation (Fulop et al., 2022), loss of synapses (Long and Holtzman, 2019; Wegmann et al., 2021), and neuron death (Crews and Masliah, 2010). Given the severity of the disease and the increasing number of patients with Alzheimer's

* Corresponding author.
** Corresponding author.
*** Corresponding author.
E-mail addresses: liusp@shu.edu.cn (S. Liu), jingtian@cxxy.seu.edu.cn (J. Tian), na.chen@shu.edu.cn (N. Chen).

https://doi.org/10.1016/j.heliyon.2022.e12366
Received 22 April 2022; Received in revised form 17 August 2022; Accepted 7 December 2022

disease, the development of effective therapies for treating AD has become a top priority. At present, the drugs that can be used for Alzheimer's disease treatment mainly include cholinesterase inhibitors and N-methyl-D-aspartate receptor antagonists (Huang et al., 2020; Ju and Tam, 2022; Long and Holtzman, 2019), but these can only suppress the symptoms of dementia for a limited time; they cannot prevent or reverse the progression of the disease. Despite many clinical studies on new drugs in recent years, the etiology and pathological changes of Alzheimer's disease remain obscure.

In addition to drug treatment, clinical treatments for Alzheimer's disease have also started adopting non-drug therapies, such as cognitive training (Huang et al., 2021) music therapy (Lai et al., 2020), daily activity training (Kudlicka et al., 2019; Lai et al., 2020), aromatherapy, exercise therapy (Huang et al., 2021), electrical stimulation (Hu et al., 2020), light stimulation (Hamblin 2016), acoustic stimulation, laser stimulation (Anders et al., 2015; Li et al., 2012), transcranial magnetic stimulation (Boggio et al., 2011; Pang and Shi, 2021), and other physical therapies, as these can be effective supplements to drug therapy for improving AD patients' symptoms. In particular, studies have shown that high-frequency repetitive transcranial magnetic stimulation (rTMS) of the precuneus (PC) can enhance cognitive performance for patients with typical AD-related cognitive function impairments, making this a promising non-invasive treatment for early AD patients (Koch et al., 2018). In other studies, a combined modality of aerobic and non-aerobic exercise has been found to positively affect brain structure and cognitive function in AD patients with mild cognitive impairment (Cheignon et al., 2018; Ju and Tam, 2022). In recent years, treatments involving integrative sensory stimulation have also received more attention, such as vision (Zhang, et al., 2015; Zibrandtsen et al., 2020), auditory, and tactile therapies. In 2019, a review article reported that cognitive stimulation, music therapy, and psychotherapy can improve depression in people with dementia, anxiety, and quality of life (Long and Holtzman, 2019). In another study, changes in gamma oscillations (20–50 Hz) have been observed in several neurological disorders, which have been observed in patients with Alzheimer's disease and specific mouse models of the disease (Iaccarino et al., 2016), however, the relationship between gamma oscillations and cellular pathologies is unclear. The Martorell team found that the combination of γ-rhythmic light scintillation and auditory stimulation can drive γ-frequency neural activity in the visual cortex, auditory cortex, and hippocampal CA1 area, enhance mitochondrial function and neural plasticity, it's given gamma oscillations' light scintillation or auditory stimulation before the onset of plaque formation or cognitive decline in a mouse model of Alzheimer's disease, but not other frequencies reduces levels of amyloid-β ($A\beta_{1\text{-}40}$ and $A\beta_{1\text{-}42}$)and improves cognition (Martorell et al., 2019). In addition, due to the absorption of light by the skin, photobiostimulation with infrared/near-infrared lasers can penetrate deeply into tissues (Castellano et al., 2012). Low-intensity laser therapy is found to enhance neuronal metabolism and stimulate neurogenesis and synaptogenesis (Li et al., 2012; Tyan et al., 2012), which is vital for neurological and psychological treatment. Overall, non-drug treatments are becoming increasingly popular due to their strong operability, safety, and acceptability by patients and their families.

Based on the Martorell team's γ-rhythm light scintillation combined with auditory stimulation, we perform multisensory stimulation on an Alzheimer's mouse model (APP/PS1 mice) using γ-rhythmic visible light, music, and infrared lasers to explore the effect of this stimulation on neurons. We take relevant behavioral experiments and hippocampal tissue in vitro experiments to determine whether they help improve APP/PS1 mice's learning, memory, and cognitive abilities.

2. Materials and methods

2.1. Animals

For this experiment, we used 40 4-month-old SPF-grade male APP/PS1 transgenic mice and 10 4-month-old wild-type male C57BL/6 mice with the same background, age, and sex, the weight of the mice was 25 ± 5 g, all mice were purchased from Beijing Weishang Lituo Technology Co., Ltd. Company (license number: SCXK (Beijing) 2016-0009). Mice were kept in a professional animal breeding room, strictly conforming to SPF animal operation specifications, where the breeding environment temperature was 25 ± 2 °C and 12 h of light and 12 h of darkness every day. Mice were given adequate food and clean water. All animals were kept in the animal room for one week to become familiar with the environment, then the experiment was carried out. The experiment project and the animals in this study were reviewed and approved by the Ethics Committee of Shanghai University (ECSHU).

The experimental animals were divided into five groups, each group with 10 mice. The C57 control group (C57 group) included wild-type 4-month-old C57BL/6 mice of the same strain as APP/PS1. The other four groups were selected from 4-month-old APP/PS1 transgenic mice and randomly divided into the APP/PS1 model control group (APP/PS1 group), the light and music intervention group (LED + music group), the laser intervention group (laser group), and the intervention group including light, music, and laser stimulation (LED + music + laser group), with 10 mice in each group. The C57 group and the APP/PS1 group mice have no intervention, the LED + music group mice need 1 h of LED and music stimulation every day, the laser group mice were given laser stimulation for 0.5 h every day, and the mice in the LED + music + laser group were given LED, music stimulation for 1 h, and laser stimulation for 0.5 h every day. After the 45-day (LED/music/laser) physical stimulation experiment, the mice were about 5 months and 3 weeks old (all animals were kept in the animal room for one week to become familiar with the environment), all experimental animals in each group need to do the Morris water maze test, open field test, and new object recognition test (the mice still received (LED/music/laser) physically stimulated during the behavioral experiments). After 7-day behavioral experiments, we choose five experimental mice from each group to detect the content of amyloid ($A\beta_{40}$ and $A\beta_{42}$) in hippocampal tissue by ELISA method and do Nissl staining for hippocampal tissue.

2.2. Experimental device design

The light stimulation device (placed on the top of the cage) is a green LED array (4 × 4) controlled by a single-chip microcomputer, with the frequency of 40Hz (LED array flickered once every 0.025 s), the light intensity of 200–300 lx (lux), the wavelength of 520–525 nm, rated voltage forge of 3.2–3.6 V, and the maximum power of 3 W (Figure 1A). The music stimulation device consists of an MP3 voice player module and loudspeaker (placed on the top of the cage), with the frequency of 40 Hz sound intensity of 60–80 dB, input voltage of 3.3 V, and the maximum power of 3 W (Figure 1B). The laser device has a wavelength of 808 nm, input voltage of 2.2–3 V, and a maximum power of 20 mW (Figure 1C).

2.3. Morris water maze test

After the intervention, each group of mice was subjected to a water maze experiment for a total of 6 days (5 days for positioning navigation; 1 day for exploring the space) to evaluate the mice's spatial learning and memory abilities. The equipment for the Morris water maze experiment includes a pool (diameter 120 cm, height 50 cm, water temperature 23 ± 2 °C), a platform (diameter 8 cm, submerged 1–2 cm underwater), a video acquisition system, and an analysis system. On the day before the experiment, the mice of each group were adapted to the pool for 10 min. The platform was visible, and there was no statistical difference between groups in the time the mice took to reach the platform and their swimming speed ($P > 0.05$). The positioning navigation test, which took place over the first 5 days, involved training 4 times a day, where each training interval was 60 s. The time was recorded for each mouse to find the hidden underwater platform (escape time). On day 6, mice underwent the space exploration experiment. In this experiment, the hidden underwater platform was removed, and the mice were put into the water

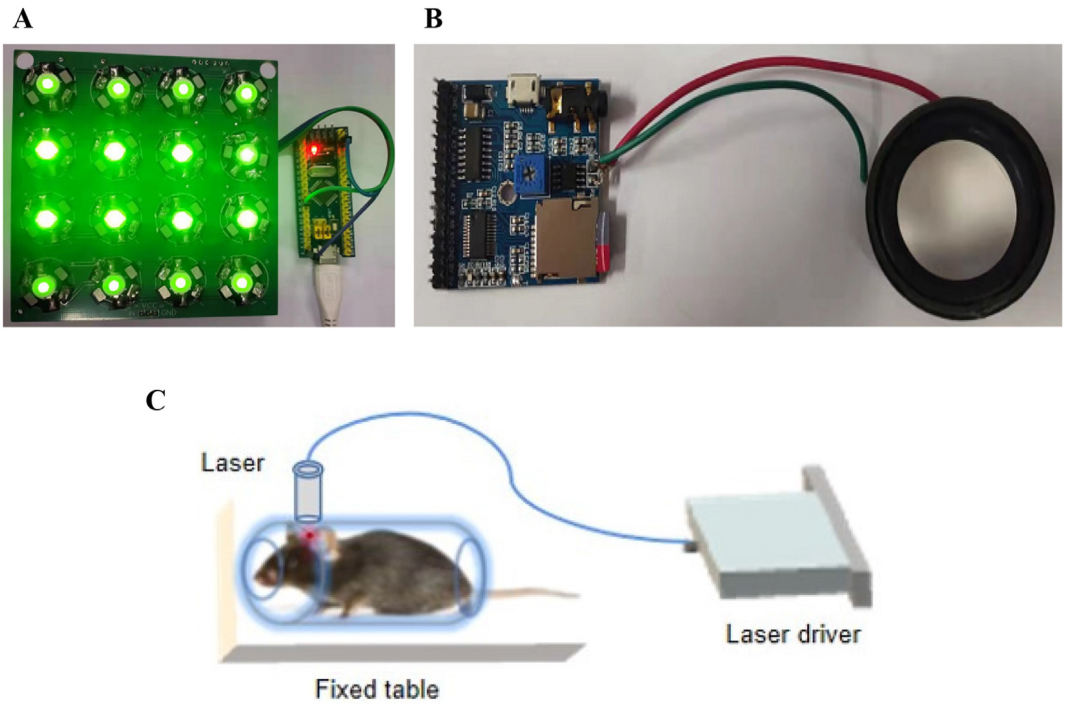

Figure 1. Experimental device design for (LED/music/laser) physical stimulation. (A) The light stimulation device. (B) The music stimulation device. (C) The laser stimulation device.

from each of the four-quadrant entry points, and we recorded the mice's swimming path, swimming speed, swimming time, and the number of times they crossed the area where the platform was previously located (D'Hooge and De Deyn, 2001; Vorhees and Williams, 2010).

2.4. Open field experiment

The equipment for the open field experiment includes a square box (40 cm × 40 cm × 40 cm), an animal behavior analysis system, and camera equipment. The bottom of the cube box is divided into 16 small squares of equal size. The four small squares in the middle are regarded as the central area, and the rest are the surrounding areas. All mice are transferred to the laboratory to allow them to adapt for 12 h, then the mice were put into the box. They were allowed to explore freely for 5 min. After the experiment was over, the bottom is sprayed with 75% alcohol and wiped with absorbent paper to prevent the residual odor from affecting the next mouse. The evaluation indicators are the total distance that each mouse moved in the open field and active time in the central area.

2.5. Novel object recognition test

Novel object recognition (NOR) is usually used for evaluating the mice's memory abilities. The memory and cognitive abilities of the mice can be assessed according to the length of time the animal explored old objects and new objects. If a mouse's memory/cognitive ability is poor, there will be no difference in the time of exploration; if a mouse's memory/cognitive ability is normal, they will explore a new object for longer than they explore an old object. The recognition index (RI) is new object/(new object + old object). The experiment procedure is including three stages: The first stage is the adaptation period, where the mouse moved freely in the experimental device (without objects) for 5 min, thus representing an open field experiment. The second stage is the familiarization period, where, within 2 h after the end of the first stage, two identical objects are placed in the device (A and A′ are the same objects, namely cylinders with a diameter of 3 cm and a height of 10 cm). The evaluation index was is the time (out of 5 min) that each mouse explored each object. The third stage is the testing period, which starts 3 h after the completion of the second stage. Here, one of the two identical objects (A or A′) is replaced with a different object B (B is a cylinder with a diameter of 3 cm and a height of 10 cm), and the mouse is placed back in the device for 5 min. The evaluation indicator is the same as in the second stage.

2.6. Hippocampus $A\beta_{40}$ and $A\beta_{42}$ level detection by ELISA

Accumulation of beta-amyloid peptide (Aβ) is highly associated with Alzheimer's disease (Manca et al., 2019; Molinuevo et al., 2020; Pickering et al., 2021). Two main types of β-amyloid peptides, namely $A\beta_{40}$ and $A\beta_{42}$, reflect the deposition of amyloid in the brain and the formation of neuroinflammatory plaques in the brain (Waragai et al., 2012; Koychev et al., 2018). After the behavioral experiments, 5 mice were randomly selected from each group the brains were harvested after chloral hydrate anesthesia, and the hippocampal tissue was separated and prepared into hippocampal tissue solution (the ratio of hippocampal tissue weight to PBS was 1:9), then the contents of $A\beta_{40}$ and $A\beta_{42}$ were detected according to the instruction of ELISA kit to eliminate the effects of the weight of the mice on Aβ level.

2.7. Nissl staining in hippocampus tissues

After chloral hydrate was used to anesthetize the mice, hippocampal tissue was removed, and the hippocampal tissue was solidified in an OCT embedding agent. The operating temperature of the cryotome (Thermo HM525) was adjusted to −22 °C. The OCT embedded tissue block was placed in the cryotome for 20–30 min to equilibrate the temperature, then serial sections and patches were performed with a thickness of 8 um. Nissl staining can stain Nissl body, used to observe the cellular structure of neurons, we can detect the damage of neurons by observing Nissl body. In this experiment, Toluidine Blue was used for staining. The staining steps were as follows: Frozen sections were fixed with 4% PFA for 15 min, washed with PBS for 2 min, and then stained with Nissl staining solution for 7 min when the tissue temperature was at 37–50 °C. Sections were washed with PBS twice, each time for 10 s, then they were washed with 95% ethanol for about 5 s. Sections were dehydrated in 95% ethanol for 2

min, then replaced with fresh 95% ethanol and dehydrated for 2 min. Xylene was transparent for 5 min, then followed by fresh xylene until the tissue was completely clear for 5 min. For the stained sections, we used neutral gum to seal the sections with cover slides, then the tissue slice can be observed under a microscope (Xie et al., 2021; Zhang et al., 2017).

2.8. Statistical analysis

The data were analyzed using statistical methods and the results were expressed as mean ± standard (x ± s). One-way analysis of variance (ANOVA) was used for comparison between multiple groups, the LSD method was used for pairwise comparisons between groups, and an independent-sample t-test was used for intra-group comparison; the difference was considered statistically significant when $P < 0.05$.

3. Results

3.1. Effects of light, music, and infrared laser stimulation on learning and memory ability

Results of the positioning navigation experiment are given in Table 1, which shows the escape latency of the five groups of mice for 5 days. On day 1 and day 2, there was no significant difference between or within groups ($P > 0.05$). On days 3–5, the escape latency of mice in each group gradually shortened. Compared with the C57 group, the escape latency of the APP/PS1 group was significantly longer. Compared with the APP/PS1 group, the escape latency of the three intervention groups decreased considerably: On day 4, compared with the APP/PS1 group, the escape latency of the LED + music group decreased significantly on day 4($P < 0.05$) and on day 5($P < 0.05$); the escape latency of the laser group decreased significantly on day 4($P < 0.05$) and day 5($P < 0.05$); the escape latency of the LED + music + laser group was further decreased on day 3($P < 0.05$), day 4($P < 0.05$), and day 5($P < 0.01$). For the five groups of mice, with the extension of the training time of the positioning and navigation experiment, the escape latency of each group of mice to find the underwater platform gradually shortened (Figure 2A), especially on days 3–5, indicated that LED, music of γ rhythm and laser stimulation can enhance the spatial learning and memory ability of APP/PS1 mice.

On the other hand, after the 5-day positioning navigation experiment, the platform was removed at the same time the next day, and the space exploration experiment was performed on day 6. We record the mice's 60-s swimming trajectory (Figure 2B) by CCD (Charge Coupled Device), the C57 group found the location of the original underwater platform more easily, while the APP/PS1 group found it more difficult. Then we evaluated the mice's spatial memory abilities via the average swimming speed, the total distance swimming, the distance swimming in the goal quadrant, and the number of platform crossings (Figure 2(C–F)). The swimming speed (Figure 2C) of the C57 group was higher than the APP/PS1 group ($P < 0.01$), while there was no significant difference between the other four groups ($P < 0.05$). Compared with the C57 group, the APP/PS1 group showed a smaller swimming distance (Figure 2D), a shorter distance swimming in the goal quadrant (Figure 2E), and a less number of platform crossings ($P < 0.01$)., 'the distance swam in the goal of the LED + music group and LED + music + laser group was significantly larger ($P < 0.05$) compared to the APP/PS1 group; the number of platform crossings in the laser group ($P < 0.05$) and LED + music + laser group ($P < 0.01$) was significantly larger than APP/PS1 group (Figure 2F), indicating that γ-frequency light, music, and infrared laser stimulation can improve the learning and memory ability of APP/PS1 mice.

3.2. Effects of light, music, and laser stimulation on exploration ability

Mice in each group were allowed to exercise in the open field for 5 min. The trajectory of each group of mice in the open field experiment was shown in Figure 3A, the C57 group showed the strongest desire to explore. We recorded and analyzed the mice in each group's moving distance (Figure 3B), average speed (Figure 3C), total activity time (Figure 3D), and time spent in the center (Figure 3E), there was no statistical difference in the moving distance, average speed, and total activity time between groups ($P > 0.5$), indicating that γ-rhythm light, music, and infrared laser stimulation did not affect the exercise ability of mice in each group. However, time spent in the center for the APP/PS1 group was significantly lower ($P < 0.01$) than that of the C57 group, indicating a significant difference in the exploration ability between the C57 group and the APP/PS1 group ($P < 0.01$), the C57 group mice were more willing to explore. Compared with the APP/PS1 group, the central activity time of the LED + music + laser group was significantly higher ($P < 0.01$), and the LED + music group showed obvious differences ($P < 0.05$). Thus, we can consider that light, music, and laser stimulation can improve the exploration ability of APP/PS1 mice.

3.3. Effects of light, music, and infrared laser stimulation on cognitive ability

The effects of γ-frequency light, music, and infrared laser stimulation on mice's ability to recognize new objects are shown in Figure 4. There were no statistical differences in the time the mice spent in recognizing two same objects (A and A′) ($P > 0.05$), indicating that all mice had no obvious preference for two same objects. However, the recognition time of the APP/PS1 group was significantly lower than C57 group, indicating that the APP/PS1 mice's desire to explore was not strong (Figure 4A). When two different objects were available (A and B), the C57 group ($P < 0.01$), the LED + music group ($P < 0.05$), and the LED + music + laser group ($P < 0.05$) had significantly higher recognition times for the new object (B) than the old object (A) (Figure 4B). In addition, compared with the C57 group, the new object recognition index (RI) for the APP/PS1 group was significantly lower ($P < 0.05$); compared with the APP/PS1 group, the RI for the LED + music + laser group ($P < 0.05$) was significantly higher (Figure 4C). These findings indicated that the APP/PS1 model mice had an impaired cognitive ability for new objects, and γ-rhythm light, music, and infrared laser stimulation could improve their cognitive ability.

3.4. Effects of light, music, and infrared laser stimulation on $A\beta_{40}$ and $A\beta_{42}$ in the hippocampus of mice

The solution concentration of $A\beta_{40}$ and $A\beta_{42}$ (ng/ml) in the suspension of hippocampal tissue and the $A\beta_{42}/A\beta_{40}$ ratio for each group

Table 1. The escape time of mice in each group during the positioning navigation phase ($\bar{x} \pm s, n = 10$).

Group	Escape time(s)				
	Day1	Day2	Day3	Day4	Day5
C57	45.24 ± 4.01	42.42 ± 3.31	29.49 ± 4.38$^{\&\&}$	27.21 ± 4.01$^{\&\&}$	22.75 ± 3.86$^{\&\&}$
APP/PS1	57.44 ± 4.32	54.21 ± 3.95	50.75 ± 3.64$^{\#\#}$	47.16 ± 3.90$^{\#\#}$	37.11 ± 3.39$^{\&\#}$
LED + music	52.24 ± 4.02	51.88 ± 2.94	47.03 ± 3.55	40.29 ± 3.18$^{\&}$	33.5 ± 3.17$^{\&*}$
Laser	55.15 ± 3.04	52.78 ± 2.83	46.06 ± 3.67	36.44 ± 3.24$^{\&*}$	32.88 ± 3.49$^{\&**}$
LED + music + laser	57.02 ± 3.29	55.37 ± 4.34	44.5 ± 4.50$^{\&}$	36.06 ± 4.28$^{\&*}$	29.98 ± 2.65$^{\&\&**}$

$^{\#}P < 0.05$, $^{\#\#}P < 0.01$ VS C57; $^{*}P < 0.05$, $^{**}P < 0.01$ VS APP/PS1; $^{\&}P < 0.05$, $^{\&\&}P < 0.01$ VS day1.

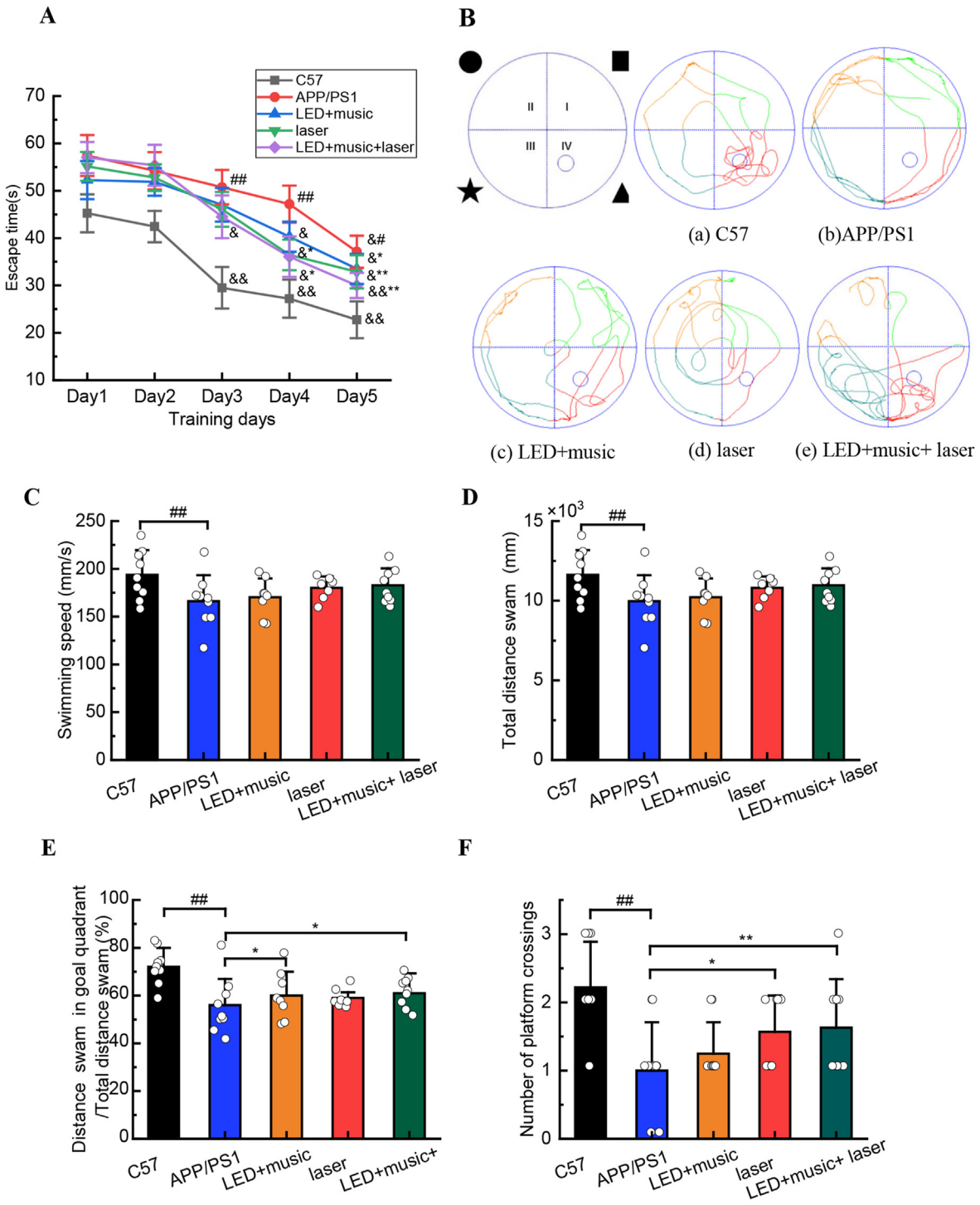

Figure 2. The results in each group during the space exploration phase. (A) The escape time of mice in each group in the positioning navigation test, where a horizontal comparison can be made within groups according to the number of learning days. (B) Representative tracks in each group. (C) The average swimming speed in each group. (D) The total distance swam in each group. (E) The distance swimming in the goal quadrant in each group (F) The number of platform crossings in each group during the space exploration phase. $^{\&}P < 0.05$, $^{\&\&}P < 0.01$ vs day1; $^{\#}P < 0.05$, $^{\#\#}P < 0.01$ vs C57 group; $^{*}P < 0.05$, $^{**}P < 0.01$ vs APP/PS1 group; Mean ± SEM, n = 10.

of mice was shown in Figure 5. By investigating multiple comparisons for the content of soluble $A\beta_{40}$ and $A\beta_{42}$ in the hippocampus, we found there was a significant difference in the level of soluble $A\beta_{40}$ and $A\beta_{42}$ between C57 group and APP/PS1 group ($P < 0.05$)ompared to the APP/PS1 group, there was a less concentration of $A\beta_{40}$ in the laser group ($P < 0.05$) and the LED + music + laser group ($P < 0.01$) (Figure 5A); there was a less concentration of $A\beta_{42}$ in the LED + music + laser group ($P < 0.05$) (Figure 5B). In addition, compared with the C57 group, the ratio of $A\beta_{40}$ to $A\beta_{42}$ in the APP/PS1 group was significantly lower ($P < 0.01$), while there was no significant difference in the other groups (Figure 5C). These findings show that the γ-rhythm light, music, and infrared laser stimulation could reduce the content of $A\beta_{40}$ and$A\beta_{42}$in the hippocampus of APP/PS1 model mice.

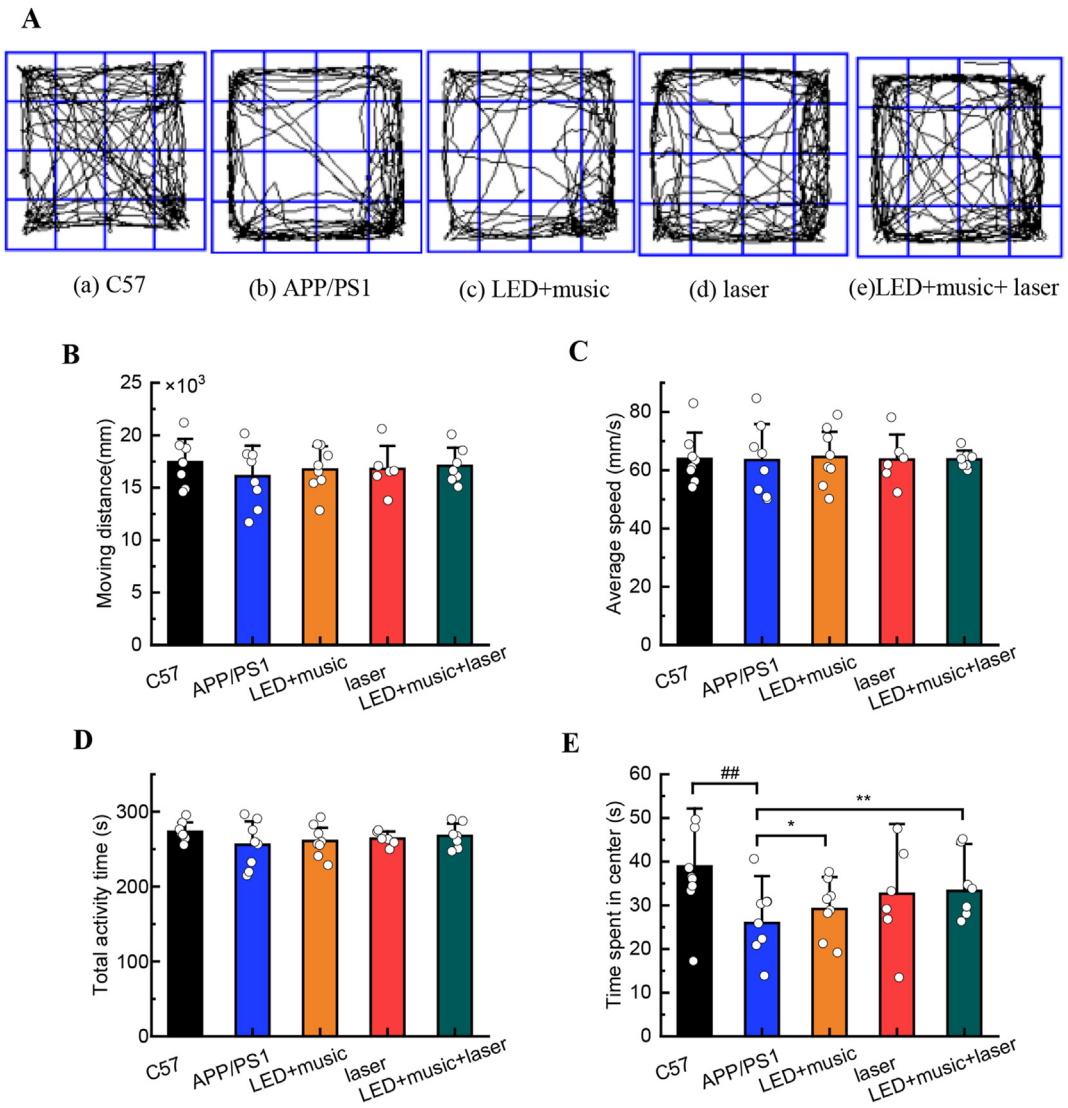

Figure 3. The results for mice in each group during the open field. (A) Representative tracks for each group. (B) The moving distance for each group. (C) Average speed for each group. (D) Total activity time for each group. (E) Time was spent in the center for mice in each group during the open field test. $^{\#\#}P < 0.01$ vs C57 group; $^{*}P < 0.05$, $^{**}P < 0.01$ vs APP/PS1 group; Mean ± SEM, n = 10.

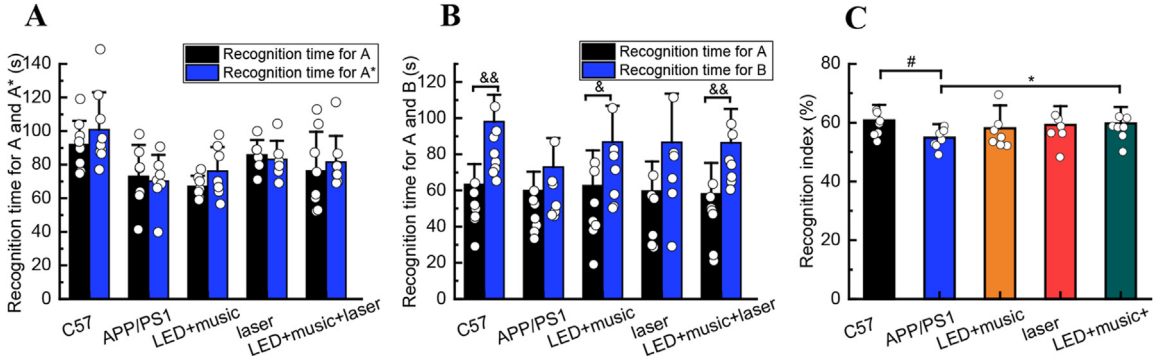

improve their cognitive ability.

Figure 4. Recognition of the same objects and different objects for mice in each group during the new object recognition. (A) The recognition time for two same objects (A and A′) between groups. (B) The recognition time for two different objects (A and B) between groups. (C) The recognition index for five groups. $^{\#}P < 0.05$, $^{\#\#}P < 0.01$ vs C57 group; $^{*}P < 0.05$, $^{**}P < 0.01$ vs APP/PS1 group. $^{\&}P < 0.05$, $^{\&\&}P < 0.01$ vs recognition time for A; Mean ± SEM, n = 10.

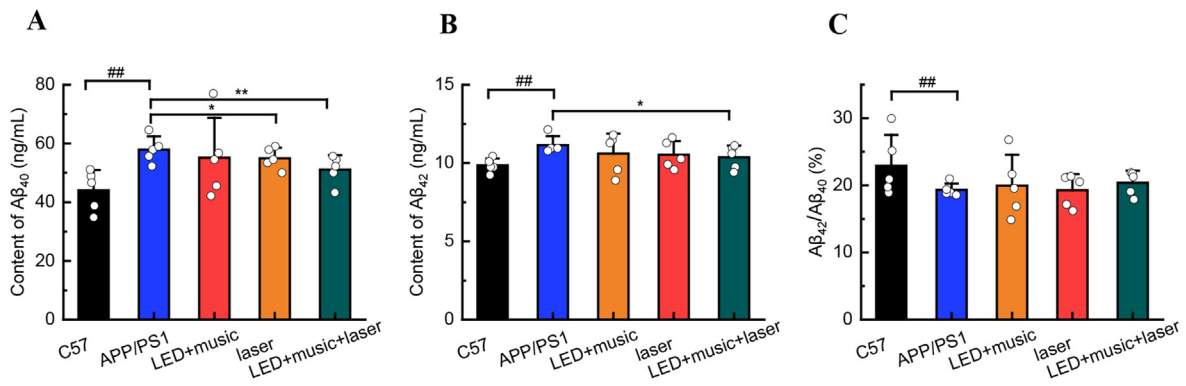

Figure 5. Effects of light, music, and infrared laser stimulation on $A\beta_{40}$ and $A\beta_{42}$ in the hippocampus of mice. (A) The solution concentration of $A\beta_{40}$ (ng/ml) in the suspension of hippocampal tissue for each group. (B) The solution concentration of $A\beta_{42}$ (ng/ml) in the suspension of hippocampal tissue for each group. (C) The ratio of $A\beta_{40}$ to $A\beta_{42}$ in the suspension of hippocampal tissue for each group. $^{\#}P < 0.05$, $^{\#\#}P < 0.01$ vs C57 group; $^{*}P < 0.05$, $^{**}P < 0.01$ vs APP/PS1 group; Mean ± SEM, n = 5.

3.5. Effect of light, music, and infrared laser stimulation on the structure of the hippocampus

The active component in the Nissl staining solution is toluidine blue, and when stained with this solution, cell bodies appear as a mottled blue-purple (Figure 6A). There showed that the neurons in the hippocampus of the C57 group were arranged neatly with darker staining, while the hippocampal neurons had a disordered arrangement with larger gaps and lighter staining in the APP/PS1 group, we speculated that there were a large number of neurons were missing (Merino-Serrais et al., 2019; Zhang et al., 2021). Using Image-Pro Plus 6.0 software to analyze the average optical density (AOD) of the stained sections (Fig. 6B-D), we found that the AOD of the CA1 area, the CA3 area, and the DG area of the hippocampus in the C57 group was higher than the AOD of the corresponding areas in the other four groups. There were higher AOD in the CA1 area in the LED + music group ($P < 0.05$), the laser group ($P < 0.05$), and the LED + music + laser group ($P < 0.01$) than APP/PS1 group; There were higher AOD in CA3 area in the LED + music group ($P < 0.05$), the laser group ($P < 0.01$), and in the LED + music + laser group ($P < 0.01$) than APP/PS1 group; There were higher AOD in CA3 area in the LED + music + laser group ($P < 0.05$) than APP/PS1 group. Thus, light, music, and infrared laser intervention may reduce neuronal loss in the hippocampus of APP/PS1 mice.

4. Discussion

Alzheimer's disease is a degenerative disease of the central nervous system, characterized by changes in cognitive function, often accompanied by abnormal behaviors such as poor memory, impaired cognitive behavior, and depressive emotion (Boggio et al., 2011; Koch et al., 2018). Clinical studies have found that the brains of AD patients with cognitive impairment have abnormal changes in γ rhythm; further, magnetoencephalogram-electroencephalogram (MEG-EEG) and transcranial magnetic stimulation-electroencephalogram (TMS-EEG) have also shown that AD patients have decreased or abnormally enhanced γ-rhythm synchrony in the resting state. In this study, to investigate whether LED, music at a γ rhythm, and infrared laser stimulation can improve memory abilities and cognitive behavior in Alzheimer's disease model mice, APP/PS1 mice were selected for physical stimulation, including γ-rhythmic visible light, music, and infrared laser. At 4 months of age, APP/PS1 mice are in the prepathological stage of AD, at which time, their brain Aβ begins to increase, but without cognitive impairment. When APP/PS1 mice are 5 months old, they show decreased spatial memory ability and began to show cognitive impairment, Aβ begins to be generated, and the content of Aβ was different from that of normal mice, but there was no senile plague yet (Lee and Han, 2013; Abulizi et al., 2015). When APP/PS1 mice are 6 months old, senile plaques appear in their brains and cognitive dysfunction occurred (Di Loreto et al., 2014; Pei et al., 2019). Based on the above analysis, 4-month-old APP/PS1 mice were selected for the experiments. To avoid the variables in the experimental environment, throughout the experiment we kept the lighting, temperature, and humidity constant in the animal room to eliminate any variables due to human factors. We also kept the breeder and the experimenter constant to ensure the reliability of the experimental data. In addition, we conducted a visual platform experiment on mice in each group before the water maze experiment, finally, all mice were able to find the platform floating on the horizontal plane. Therefore, all mice had no differences in eyesight, which ensured the accuracy of the experimental data. In the behavioral experimental results, γ-rhythmic LED, music, and infrared laser stimulation can improve the memory ability and cognitive behavior of APP/PS1 mice, especially the combination of LED, music, and infrared laser stimulation. However, it is worth noting that there was a significant difference in the swimming speed between the C57 group and the APP/PS1 group in the Morris water maze experiment, while there was no statistical difference in the movement speed in the open field experiment, therefore, we speculated that APP/PS1 mice were more prone to fatigue during swimming. On the other hand, the cause of AD has always been a mystery, among the many hypotheses, the amyloid beta (Aβ) cascade hypothesis is the most accepted, amyloid precursor protein (APP) is cleaved to form amyloid (Aβ), and Aβ aggregates to form oligomers, leading to neurofibrillary tangles and neuronal loss. Some studies have shown that the decrease of soluble Aβ42 is highly correlated with AD symptoms. Therefore, soluble Aβ40 and soluble Aβ42 were selected for ELISA detection, while we did not reject the research value of insoluble Aβ. By comparing the C57 group and APP/PS1 group, the content of $A\beta_{42}$, $A\beta_{40}$, and the ratio of ß42 to ß40 in the APP/PS1 group was significantly higher than C57 group ($P < 0.01$), which indicated that APP/PS1 mice were indeed able to successfully simulate the pathological characteristics of AD. By comparing the contents of soluble Aβ40 and Aβ42 in the hippocampus of APP/PS1 mice, the soluble Aβ40 was decreased ($P < 0.05$) only in the LED + music + Laser group, and the soluble Aβ42 also decreased in the laser group ($P < 0.05$) and LED + Music + Laser group ($P < 0.01$), however, the ratio of Aß42 to $A\beta_{40}$ had little difference ($P > 0.05$), which indicate that the decrease of soluble $A\beta_{42}$ is highly correlated with AD, while γ-rhythm LED, music and infrared laser stimulation can reduce the content of $A\beta_{42}$ in the hippocampus of APP/PS1 mice. Compared with APP/PS1 group, the AOD of hippocampal sections in the LED + music group, laser group, and LED + music + laser group increased to varying degrees, indicating that neuronal apoptosis was reduced. We can indicate that the combined

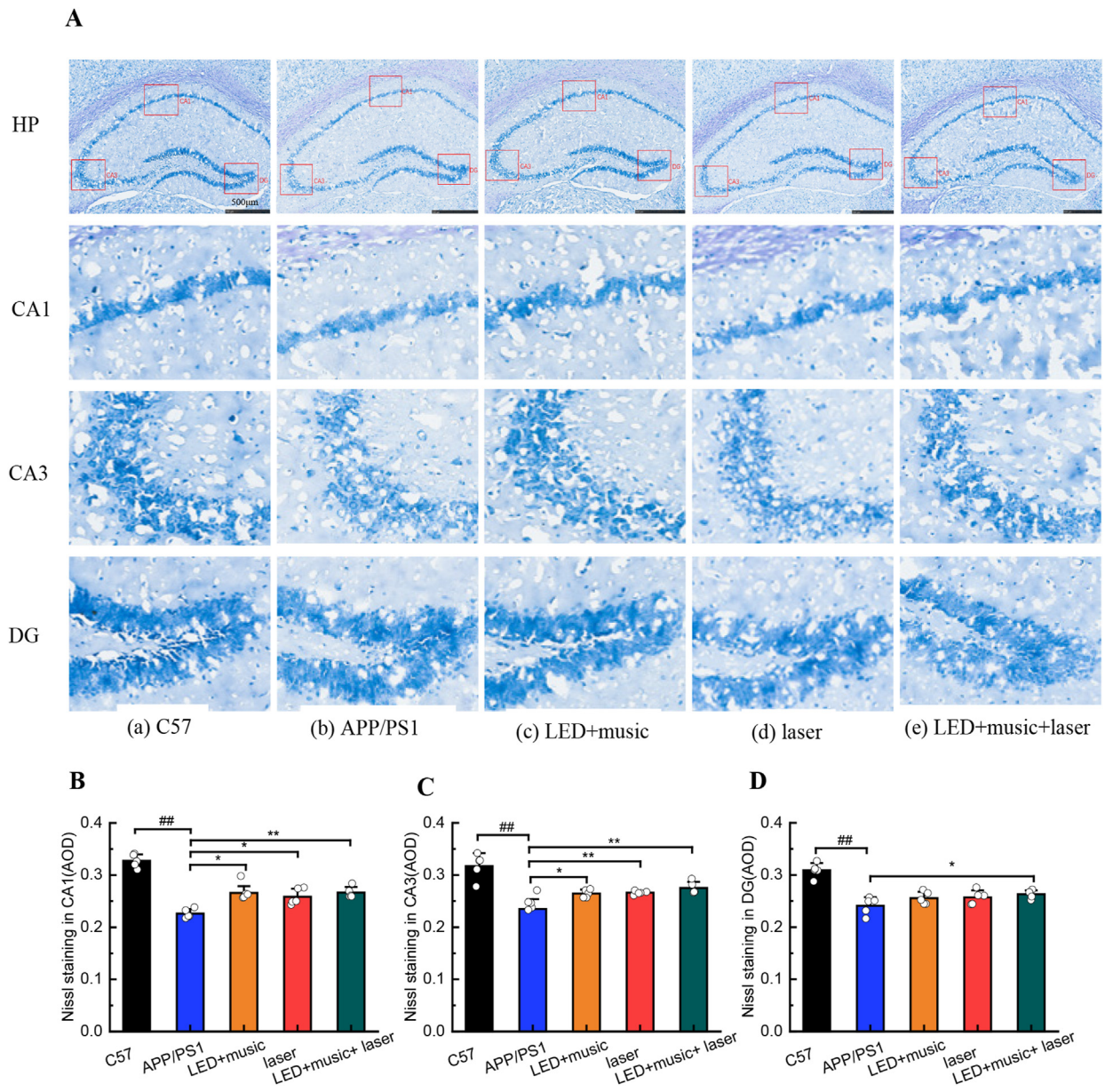

Figure 6. Effect of light, music, and infrared laser stimulation on the structure of the hippocampus in mice. (A) Representative results of Nissl staining, show changes in the hippocampal neurons in each group. (B) The AOD of Nissling staining in the CA1 area. (C) The AOD of Nissling staining in the CA3 area. (D) The AOD of Nissling staining in the DG area. $^{\#}P < 0.05$, $^{\#\#}P < 0.01$ vs C57 group; *P < 0.05, **P < 0.01 vs APP/PS1 group; Mean ± SEM, n = 5; The scale is 500 μm.

intervention of γ-rhythm visible light, music and infrared laser stimulation can reduce neuronal loss in the hippocampus of APP/PS1 mice.

In summary, combined γ-rhythm visible light, music, and infrared laser stimulation delivered were able to improve the APP/PS1 mice's memory abilities and cognitive behavior, reduce the Aβ and improve the apoptosis of neuronal cells in the hippocampus. From the overall effect analysis, the comprehensive effect of LED + music + laser stimulation was better than LED + music stimulation or only infrared laser stimulation. There still exist shortcomings in the study, we have not performed adequate physical stimulation experiments for frequency, light intensity, sound intensity, and power due to insufficient experimental animals, furthermore, we only tested endogenous amyloid in mice but not measured human Abeta, the mechanistically complex interaction of human and mouse Aβ may affect the pathogenesis of the models and should be considered when models are used for translational preclinical studies. our follow-up studies aim to further explore the therapeutic effect of combined stimulation with γ-rhythm light, music, and infrared lasers on patients with Alzheimer's disease.

5. Conclusion

In conclusion, through the analysis of physical stimulation (LED/music/laser)) on APP/PS1 mice based on animal behavior and pathology experiments, the study indicated the neuroprotective effect of combined γ-rhythm light, music, and infrared laser stimulation in AD. Our results suggest that multi-model (LED/music/laser) physical stimulation on APP/PS1 mice is more effective in relieving AD symptoms than single laser stimulation or light and music stimulation. Overall, our study offers a theoretical basis for using γ-rhythm LED, music, and infrared laser stimulation in clinical AD prevention and treatment.

Declarations

Author contribution statement

Shupeng Liu, Shuyang Li: Conceived and designed the experiments; Performed the experiments; Analyzed and interpreted the data; Wrote the paper.

Yudan Xia, Heng Zhang: Performed the experiments; Contributed reagents, materials, analysis tools or data; Wrote the paper.

Jing Tian, Chunlei Shan, Ying Wang: Performed the experiments; Contributed reagents, materials, analysis tools or data.

Fufei Pang, Yana Shang, Na Chen: Conceived and designed the experiment; Analyzed and interpreted the data.

Funding statement

This work is supported by the National Natural Science Foundation of China (62175142 and 61875118) and Shanghai Clinical Research Center for Rehabilitation Medicine (21MC1930200). The authors would like to thank the support of the 111 Project (D20031).

Data availability statement

Data included in article/supp. material/referenced in article.

Declaration of interest's statement

The authors declare no conflict of interest.

Additional information

No additional information is available for this paper.

Acknowledgements

All institutional and national guidelines for the care and use of laboratory animals were followed. The experiments comply with the current laws of the country in which they were performed.

References

Abulizi, J., Wang, X., Li, F., et al., 2015. Effect of electro-acupuncture intervention on hippocampus Aβ stain and ultrastructure in APP/PS1 double transgenic rats. Global Traditional Chinese Medicine 8 (5), 518–522.

Anders, J.J., Lanzafame, R.J., Arany, P.R., 2015. Low-level light/laser therapy versus photobiomodulation therapy. Photomed Laser Surg 33, 183–184.

Beyreuther, K., Masters, C.L., 1991. Amyloid precursor protein (APP) and BZA4 amyloid in the etiology of Alzheimer's disease: precursor-product relationships in the derangement of neuronal function. Brain Pathol. 1, 241–251.

Boggio, P.S., Valasek, C.A., Campanha, C., Giglio, A.C.A., Baptista, C., Lapenta, O.M., Fregni, F., 2011. Non-invasive brain stimulation to assess and modulate neuroplasticity in Alzheimer's disease. Neuropsychol. Rehabil. 21, 703–716.

Castellano, J.M., Deane, R., Gottesdiener, A.J., Holtzman, D.M., 2012. Low-density lipoprotein receptor overexpression enhances the rate of brain-to-blood Aβ clearance in a mouse model of β-amyloidosis. P Natl Acad Sci USA 109, 15502–15507.

Chan, K.Y., Wang, w, Wu, J.J., Liu, L., Theodoratou, E., car, J., Middleton, L., Russ, T.C., Deary, L.J., Campbell, H., Wang, W., Rusan, L., 2013. Epidemiology of Alzheimer's disease and other forms of dementia in China, 1990-2010: a systematic review and analysis. Lancet 381, 2016–2023.

Cheignon, C., Tomas, M., Bonnefont-Rousselot, D., Faller, C., Hureau, C., Collin, C., Collin, F., 2018. Oxidative stress and the amyloid-beta peptide in Alzheimer's disease. Redox Biol. 14, 450–464.

Chiavellini, P., Canatelli-Mallat, M., Lehmann, M., Goya, R., Morel, G., 2022. Therapeutic potential of glial cell line-derived neurotrophic factor and cell reprogramming for hippocampal-related neurological disorders. Neural Regen Res 17, 469.

Crews, L., Masliah, E., 2010. Molecular mechanisms of neurodegeneration in Alzheimer's disease. Hum. Mol. Genet. 19, 1–41.

Di Loreto, S., Falone, S., D'Alessandro, A., Santini Jr., S., Sebastiani, P., Cacchio, M., Amicarelli, F., 2014. Regular and moderate exercise initiated in middle age prevents age-related amyloidogenesis and preserves synaptic and neuroprotective signaling in mouse brain cortex. Exp. Gerontol. 57, 57–65.

D'Hooge, R., De Deyn, P.P., 2001. Applications of the Morris water maze in the study of learning and memory. Brain Res. Rev. 36, 60–90.

Fonseca, E.A., Lafetá, L., Cunha, R., Miranda, H., Campos, J., Medeiros, H.G., Romano-Silva, M.A., Silva, R.S., Barbosa, A.S., Vieira, R.P., Malard, L.M., Jorio, A., 2019. A fingerprint of amyloid plaques in a bitransgenic animal model of Alzheimer's disease obtained by statistical unmixing analysis of hyperspectral Raman data. Analyst 144, 7049–7056.

Fulop, T., Larbi, A., Khalil, A., Plotka, A., Laurent, B., Ramassamy, C., Bosco, N., Hirokawa, K., Frost, E.H., Witkowski, J.M., 2022. Immunosenescence and Alzheimer's disease. Healthy Ageing and Longevity 16, 177–199.

Guo, T.T., Zhang, D.H., Zeng, Y.Z., Huang, T.Y., Xu, H.X., Zhao, Y.J., 2020. Molecular and cellular mechanisms underlying the pathogenesis of Alzheimer's disease. Mol. Neurodegener. 15, 1–37.

Haass, C., Selkoe, D.J., 2007. Soluble protein oligomers in neurodegeneration: lessons from the Alzheimer's amyloid β-peptide. Nat. Rev. Mol. Cell Biol 8, 101–112.

Hamblin, M.R., 2016. 2016. Shining light on the head: photobiomodulation for brain disorders. BBA Clinical 6, 113–124.

Hampel, H., Caraci, F., Cuello, A.C., Caruso, G., Nistico, R., Corbo, M., Baldacci, F., Toschi, N., Garaci, F., Chiesa1, 1P.A., Verdooner, S.R., Akman-Anderson, L.L., Hernández, F., Ávila, J., Emanuele, E., Valenzuela, P.L., Lucía, A., Watling, M., Imbimbo, B.P., Vergallo, A., Lista, S., 2020. A path toward precision medicine for neuroinflammatory mechanisms in Alzheimer's disease. Front. Immunol 11, 1–24.

Holtzman, D.M., Morris, J.C., Goate, A.M., 2011. Alzheimer's disease: the challenge of the second century. Sci Transl Med 3, 1–35.

Hu, M., Hong, L., He, S.M., Huang, G.T., Cheng, Y.X., Chen, Q., 2020. Effects of electrical stimulation on cell activity, cell cycle, cell apoptosis and β-catenin pathway in the injured dorsal root ganglion cell. Molecular Med. Rep. 21, 2385–2394.

Huang, L.K., Chao, S.P., Hu, C.J., 2020. Clinical trials of new drugs for Alzheimer disease. J. Biomed. Sci. 27, 1–13.

Huang, X.X., Zhao, X.Y., Cai, Y., Wang, Q.Q., 2021. The cerebral changes induced by exercise interventions in people with mild cognitive impairment and Alzheimer's disease: a systematic review. Arch Gerontol Geriatr 98, 1–9.

Iaccarino, H.F., Singer, A.C., Martorell, A.J., Rudenko, A., Gao, F., Gillingham, T.Z., Mathys, H., Seo, J., Kritskiy, O., Abdurrob, F., Adaikkan, C., Canter, R.G., Rueda, R., Brown, E.N., Boyden, E.S., Tsai, L.H., 2016. Gamma frequency entrainment attenuates amyloid load and modifies microglia. Nature 540 (7632), 230–235.

Jack, C.R., Bennett, D.A., Blennow, K., Carrillo, M.C., Dunn, B., Haeberlein, S.B., Holtzmang, D.M., Jagusth, W., Jesseni, F., Karlawishj, J., Liuk, E., Molinuevol, J.L., Montinem, T., Phelpsn, C., Rankino, K.P., Rowep, C.C., Scheltensq, P., Siemersr, E., Snyderd, H.M., Sperlings, R., 2018. NIA-AA Research Framework: toward a biological definition of Alzheimer's disease. Alzheimer's and Dementia 14, 535–562.

Ju, Y., Tam, K., 2022. Pathological mechanisms and therapeutic strategies for Alzheimer's disease. Neural Regen Res 17, 543–549.

Koch, G., Bonnì, S., Pellicciari, M.C., Acasula, E.P., Mancini, M., Esposito, R., Ponzo, V., Picazio, S., Lorenzo, F.D., Serra, L., Motta, C., Maiella, M., Marra, C., Cercignani, M., Martorana, A., Caltagirone, C., Bozzali, M., 2018. Transcranial magnetic stimulation of the precuneus enhances memory and neural activity in prodromal Alzheimer's disease. Neuroimage 169, 302–311.

Koychev, I., Galna, B., Zetterberg, H., Lawson, J., Zamboni, G., Ridha, B.H., James, B., Rowek, J.B., Thomasb, A., Howardl, R., Malhotram, P., Ritchien, C., Lovestonea, S., Rochester, L., 2018. Aβ42/Aβ40 and Aβ42/Aβ38 ratios are associated with measures of gait variability and activities of daily living in mild Alzheimer's disease: a pilot study. Int J Alzheimers Dis 65, 1377–1383.

Kudlicka, A., Martyr, A., Bahar-Fuchs, A., Eoods, B., Clare, L., 2019. Cognitive rehabilitation for people with mild to moderate dementia. Cochrane Database Syst. Rev. 3, 1–289.

Lai, X., Wen, H., Li, Y., Li, Y., Lu, L.M., Tang, C.Z., 2020. The comparative efficacy of multiple interventions for mild cognitive Impairment in Alzheimer's Disease. A Bayesian Network Meta-Analysis 12, 1–12.

Lamb, S.E., Mistry, D., Alleyne, S., Atherton, N., Brown, D., Copsey, B., Dosanjh, S., Finnegan, S., Fordham, B., Griffiths, F., Hennings, S., Khan, L., Khan, K., Lall, R., Lyle, S., Nichols, V., Petrou, S., Zeh, P., Sheehan, B., 2018. Aerobic and strength training exercise program for cognitive impairment in people with mild to moderate dementia: the DAPA RCT. Health Technol Assess (Rockv) 22, 1–201.

Lane, C.A., Hardy, J., Schott, J.M., 2018. Alzheimer's disease. Eur J Neurol 25, 59–70.

Lee, J.E., Han, P.L., 2013. An update of animal models of Alzheimer disease with a reevaluation of plaque depositions. Exp Neurobiol 22 (2), 84–95.

Li, D., Zhang, J., Li, X., 2020. Insights into lncRNAs in Alzheimer's disease mechanisms. RNA Biol 18, 1–11.

Li, M., Yang, X., Ren, J.S., Qu, K.G., Qu, X.G., 2012. Using graphene oxide high near-infrared absorbance for photothermal treatment of Alzheimer's disease. Adv. Mater 24, 1722–1728.

Long, J.M., Holtzman, D.M., 2019. Alzheimer disease: an update on pathobiology and treatment strategies. Cell 179, 312–339.

Manca, C., Rivasseau, J.T., Roch, V., Marie, P.Y., Karcher, G., Lamiral, Z., Malaplate, C., Verger, A., 2019. Amyloid PETs are commonly negative in suspected Alzheimer's disease with an increase in CSF phosphorylated-tau protein concentration but an Aβ42 concentration in the very high range: a prospective study. J. Neurol. 266, 1685–1692.

Martorell, A.J., Paulson, A.L., Suk, H., Abdurrob, F., Drummond, G.T., Guan, W., Young, J.Z., Kim, D.N.W., Kritskiy, O., Barker, S.J., Mangena, V., Prince, S.M., Brown, E.N., Chung, K., Boyden, E.S., Singer, A.C., Tsai, L.H., 2019. Multi-sensory gamma stimulation ameliorates Alzheimer's-associated pathology and improves cognition. Cell 177, 256–271.

Merino-Serrais, P., Loera-Valencia, R., Rodriguez-Rodriguez, P., Parrado-Fernandez, C., Ismai, M.A., Maioli, S., Matute1, E., Jimenez-Mateos, E.M., Björkhem, I., DeFelipe, J., Cedazo-Minguez, A., 2019. 27-Hydroxycholesterol induces aberrant morphology and synaptic dysfunction in hippocampal neurons. Cereb. Cortex 29, 429–446.

Molinuevo, J.L., Milà-Alomà, M., Salvadó, G., Gispert, J.D., Grau-Rivera, O., Sala-Vila, A., Sánchez-Benavides, G., Arenaza-Urquijo, E., González-de-Echávarri1, J.M., Simon, M., Gwendlyn Kollmorgen, G., Zetterberg, H., Blennow, K., Suárez-Calvet, M., Study, A., 2020. Emerging beta-amyloid pathology is associated with tau, synaptic, neurodegeneration and gray matter volume differences. Alzheimers Dement 16, 1–3.

Pang, Y.F., Shi, M.F., 2021. Repetitive transcranial magnetic stimulation improves mild cognitive impairment associated with Alzheimer's disease in mice by modulating the mir-567/neurod2/psd95 axis. Neuropsychiatr Dis Treat 17, 2151–2161.

Pei, Y.N., Yang, G., Zhang, L., Gao, Y.S., Zhang, S.J., Feng, S.N., Zhou, Y.G., Zhang, X.T., Xue, W.G., 2019. Effects of electroacupuncture at Baihui and Yongquan on LC3 in brains in four-month-old APP/PS1 transgenic mice. World Sci. Technol. Modernization Traditional Chin. Med. 21 (2), 307–312.

Pickering, J., Wong, R., Al-Salami, H., Lam, V., Takechi, R., 2021. Pharmaceutical research, 2021. Cognitive deficits in type-1 diabetes: aspects of glucose, cerebrovascular and amyloid involvement. Pharm. Res. 38, 1477–1484.

Tyan, S.H., Shih, A.Y.J., Walsh, J.J., Jessica, J., Maruyama, H., Sarsoza, F., Kua, L., Eggerta, S., Hofb, P.R., Kooa, E.K., Dickstein, D.L., 2012. Amyloid precursor protein (APP) regulates synaptic structure and function. Mol. Cell. Neurosci 51, 43–52.

Vorhees, C.V., Williams, M.T., 2010. Morris water maze: procedures for assessing spatial and related forms of learning and memory. Neurology 1, 848–858.

Waragai, M., Yoshida, M., Mizoi, M., Saiki, R., Kashiwagi, K., Takagi, K., Araif, H., Tashirog, J., Hashimotoh, M., Iwaia, N., Uemuraa, K., Igarashi, K., 2012. Increased protein-conjugated acrolein and amyloid-β40/42 ratio in plasma of patients with mild cognitive impairment and Alzheimer's disease. Int. J. Alzheimers Dis. 32, 33–41.

Wegmann, S., Biernat, J., Mandelkow, E., 2021. The Authors, A current view on Tau protein phosphorylation in Alzheimer's disease. Curr. Opin. Neurobiol 69, 131–138.

Xie, Y., Yan, B., Hou, M., Zhou, M., Liu, C., Sun, M., 2021. Erzhi pills ameliorate cognitive dysfunction and alter proteomic hippocampus profiles induced by d -galactose and Aβ 1– 40 injection in ovariectomized Alzheimer's disease model rats. Pharm Biol 59, 1402–1414.

Zibrandtsen, I.C., Agger, M., Kjaer, T.W., 2020. Gamma entrainment in a large retrospective cohort: implications for photic stimulation therapy for Alzheimer's disease. J. Alzheimer's Disease 75 (4), 1181–1190.

Zhang, S., Wang, X., Ai, S., Quyang, W., Le, Y., Tong, J.B., 2017. Sepsis-induced selective loss of NMDA receptors modulates hippocampal neuropathology in surviving septic mice. PLoS ONE 12, 1–15.

Zhang, Y., Wang, F., Luo, X., Wang, L., Sun, P., Wang, M., Jiang, Y.S., Zou, J.Y., Uchiumi, O., Yamamoto, R., Sugai, T., Yamamoto, K., Kato, N., 2015. Cognitive improvement by photic stimulation in a mouse model of Alzheimer's disease. Curr Alzheimer Res 12 (9), 860–869.

Zhang, Z.H., Ba, i H., Ma, X.Y., Shen, M.L., Li, R.Q., Qiu, D., Li, S.Y., Li, G., 2021. Blockade of the NLRP3/caspase-1 axis attenuates ketamine-induced hippocampus pyroptosis and cognitive impairment in neonatal rats. J. Neuroinflammation 18, 1–12.